Title

INVESTIGATION OF Y0* (1405) PRODUCTION BY K- AT REST IN EMULSION

Authors

Barbaro-Galtieri, A.
Smith, F.M.
Patrick, J.W.

Publication Date

1963-04-08

UCRL-10641

University of California

Ernest O. Lawrence Radiation Laboratory

INVESTIGATION OF Y_0^* (1405) PRODUCTION BY K^- AT REST IN EMULSION

DISCLAIMER

Submitted for pub. in Physics Letters

UCRL-10641

UNIVERSITY OF CALIFORNIA
Lawrence Radiation Laboratory
Berkeley, California

Contract No. W-7405-eng-48

INVESTIGATION OF Y_0^* (1405) PRODUCTION BY K^- AT REST IN EMULSION

A. Barbaro-Galtieri, F. M. Smith, and J. W. Patrick

April 8, 1963

UCRL-10641

INVESTIGATION OF Y_0^* (1405) PRODUCTION BY K^- AT REST IN EMULSION

A. Barbaro-Galtieri, F. M. Smith, and J. W. Patrick

Lawrence Radiation Laboratory
University of California
Berkeley, California

April 8, 1963

A T = 0 $\Sigma\pi$ resonant state at 1405 MeV, Y_0^* (1405), has been observed in various bubble chamber experiments.[1-3] In nuclear emulsion, Eisenberg et al.[4] found that the $\Sigma\pi$ effective mass distribution showed a strong enhancement around 1405 MeV; Frisk and Ekspong[5] reported a peak in the p distribution ($\underset{\sim}{p} = \underset{\sim}{p}_\Sigma + \underset{\sim}{p}_\pi$) at a value corresponding to a mass of 1405 MeV in the $\Sigma\pi$ system produced in C^{12} in the reaction $K^- + C^{12} \rightarrow \Sigma^\pm + \pi^\mp + B^{11}$. Both experiments analyze interactions produced by K^- at rest. Because of statistical limitations no information on the spin and parity of the Y_0^* is yet known, but its width has been given. The bubble chamber experiments of Alexander et al.[2] and Alston et al.[3] yield a full width at half maximum of $\Gamma = 35 \pm 5$ and $\Gamma = 50$ MeV, respectively. Frisk and Ekspong[5] seem to observe a width of ≈ 1 MeV. The reason for this disagreement could be found in the fact that the two techniques have different resolution in energy. In our experiment we used two large stacks of emulsion where the energy resolution is ≈ 1 MeV. The $\Sigma\pi$ mass spectrum obtained for K^- interaction in C^{12} shows prominent enhancement in the region around 1412 MeV. However, using an impulse model to calculate the expected distribution for direct $\Sigma\pi$ production, we can explain the observed results without appeal to Y_0^* (1405) production. We do not confirm the 1 MeV width for the Y_0^* (1405) resonance.

Two large emulsion stacks were exposed to the K^- beam from the Bevatron. The K^- were brought to rest in the central part of the stacks and a large percentage of secondary particles came to rest in the emulsion. A sample of 270 events that showed $\Sigma\pi$ production has been analyzed. The criteria in selecting this sample were: (a) the K^- interacted at rest, (b) the π came to rest in the stack and (c) if the Σ decayed in flight, the secondary stopped in the stack. With these criteria the events not used were those where the π mesons were either steep or flat and left the stack or interacted in flight. These criteria do not introduce any bias because for K^- at rest the distribution of prongs is expected to be isotropic. Eight measurements of each dip angle were made. All angles and all Σ ranges have been measured by at least two people. The pion ranges were measured once. For all the steep tracks distortion measurements have been made to correct the dip and projected angles, but this correction did not change the angle between the Σ and the π by more than 0.5 deg. Our programs for the IBM 650 calculated for each event the total momentum ($\underset{\sim}{p} = \underset{\sim}{p}_\Sigma + \underset{\sim}{p}_\pi$), the invariant mass of the $\Sigma\pi$ system M [$M^2 = (E_\pi + E_\Sigma)^2 - (\underset{\sim}{p}_\Sigma + \underset{\sim}{p}_\pi)^2$] and the appropriate errors. The average error in p was 1.9 MeV/c and never exceeded 3.5 MeV/c. The average error in M was 1.0 MeV and $(\Delta M)_{max}$ was 1.9 MeV.

Of the 270 events analyzed, 32 had additional prongs with a length shorter than that for a 30 MeV proton, which is the limit for evaporation prongs. This small sample of events with more than 2 prongs has been measured only for comparison. An attempt has been made to select from

the 2-prong events those in which the K capture was on C^{12}. This selection is merely based on the possibility of detecting the recoiling nucleus, which is often difficult. The events have been divided into 4 categories based upon the appearance of the star center, i.e., those showing (a) recoil, (b) blob(s), (c) electron(s), and (d) clean star center. In fig. 1a the recoil events are plotted on a scatter diagram with M^2 (square of the invariant mass of the $\Sigma\pi$ system) and p (total momentum squared) as coordinates. In fig. 1b the remaining events are plotted together using different symbols for the three categories. The straight lines are kinematical relations between p^2 and M^2 for different nuclei.*
The selection criteria are the following:

(a) For each event the dip and projected angle of the recoil have been calculated from the relation $\underset{\sim}{p} = -(\underset{\sim}{p}_{\Sigma} + \underset{\sim}{p}_{\pi})$; also from p, we calculated the length by assuming the B^{11} mass for the recoil and using the range-energy relation of Heckman et al.$^{6)}$. All the events were then checked under high magnification for agreement with the calculated quantities. Those recoil events with projected angles within 10° of the calculated values and dip angles of the right order of magnitude were accepted if the

---

* Actually they are calculated by applying energy-momentum conservation to the process $K^- + N \rightarrow \Sigma + \pi + N'$, where N and N' are nuclei in their ground states differing in atomic number by unity. Lines are shown only for C, O, Br, and Ag which are the most frequent nuclei in emulsion. The nucleus N' is often left in an excited state and in that case the corresponding line is shifted to the left. In fig. 1a are shown lines for B^{11} in some of the excited states; B_9^{11} corresponds to that energy sufficient to allow $B^{11} \rightarrow Li^7 + \alpha$.

recoil lengths were in agreement with the calculated ones. The expected lengths are $L \leq 5\,\mu$. Since the mean diameter of a grain in K5 emulsions is $0.4\,\mu$, we do not expect our recoil criteria to be faultless for recoils with $L < 0.8\,\mu$ (2 grains) which corresponds to $p = 100$ MeV/c. For $p < 60$ MeV/c and a large calculated dip angle the recoil is not expected to have a detectable range, therefore such events with a clean star center have been accepted. Six of these events were added to the recoil sample. This <u>a posteriori</u> method of selecting the recoil events has been adopted in order to have a bias-free sample. In fact, it is often difficult to decide whether there is a recoil, a blob, or an electron, especially for length $< 1.5\,\mu$. On the other hand, the probability for an electron to have the same length and direction expected for the recoil of a given event is small.

(b) Included in the category of blob events were those with more than one grain at the star center or those with a single grain not satisfying the calculated recoil criteria. Part of the events on O^{16} or heavy nuclei are included in this category, because they have shorter recoils than expected for B^{11}.

(c) The electron events were those with recognizable slow electrons or those with 2 or 3 grains which were directional but did not satisfy the criteria for recoils. This category may contain events on O^{16}, for which the recoil direction is the same as for C^{12}, but whose length is shorter.

(d) The clean events were those with no visible electron, recoil or blob and with a $p > 60$ MeV/c. Satisfying these criteria were only 16 events out of 218 with $p > 60$ MeV/c. This means that we expect only 1.4 events with $p > 60$ MeV/c to be in this category rather than among the recoils.

Table I summarizes the separation of events into different categories.

Table I. Number and type of events.

Type	Recoil	Blobs	Electrons	Clean	> 2 prongs	Total
No. ev.	133	43	45	17	32	270

In fig. 1 we note the following:

(1) The recoil events lie between the line for O^{16} and the line corresponding to the last excited state for B^{11} (for which the excitation energy is enough to give $B^{11} \rightarrow Li^7 + \alpha$). In this sample we are confident that the majority of the reactions are on C^{12}. In fact the N^{15} range-energy relation is appreciably different from that of B^{11} for $p > 100$ MeV/c. There doubtless remains some O^{16} contamination, especially at low momenta, but its effect on our interpretation of the process under study is negligible.

(2) The > 2 prong events lie far from the solid lines in fig. 1b. These interactions are those in which a heavy nucleus has been left in an excited state and the excitation energy was enough to allow an evaporation prong, or those in which the π or the Σ had a secondary interaction on a proton. Heavy nuclei are most likely to give such events because of the large density of nucleons.

(3) Some 70% of the blob, electron, or clean events lie near the solid lines in fig. 1b. Many of them are probably interactions on O^{16} (from the way they have been selected). The remaining 30% show a distribution similar to that of the > 2 prong events.

In the following we shall restrict our analysis to the recoil events only. In fig. 1a the mass 1405 MeV area does not show any particular enhancement; a peak seems to occur at 1412 MeV. It is evident that the B^{11} is often left in an excited state; indeed, the distribution of points indicates excited states are preferred. From our diagram this means that for Y_0^* production in C^{12} we do not expect a peak in the p^2 distribution because different excited states give different p^2 values corresponding to a 1405 MeV invariant mass ($M^2 = 1.974\ \text{BeV}^2$). Since the position of the peak observed by Frisk and Ekspong is at $p = 170$ MeV/c, all their events would correspond to Y_0^* production in the B^{11} ground state. In fig. 2 the momentum distributions are plotted (a) for all our sample of 2-prong events and (b) for the 133 interactions on C^{12}. The distributions do not present any evidence of peaking at any particular p value.

It is very important to include among the interactions on C^{12} those events with $p < 100$ MeV/c. We may have contamination from interactions on O^{16}, but if we had not taken such events our M distribution would have had a non-negligible bias. In fig. 3 we plot the M distributions for (a) all the 2-prong events, and (b) the interactions on C^{12}. In the latter the dotted-line distribution represents the distribution we would have if we had not taken any events with $p < 100$ MeV/c. As we can see in this case we have a symmetrical distribution around 1405 MeV which could easily simulate a resonance. The M distribution in fig. 3a does not differ substantially from the one observed by Eisenberg et al.4) This distribution can be easily interpreted as that expected for direct $\Sigma\pi$ production.

An impulse model, as suggested by Block,7) has been calculated for the reaction

$$K^- + C^{12} \rightarrow \Sigma^{\pm} + \pi^{\mp} + B^{11} . \quad (1)$$

It assumes that the capture takes place on a single nucleon and neglects final-state interactions. It has been calculated for K^- captures in s, p, and d states. The wave function for the nuclear density distribution in C^{12} was assumed to be the same as the charge distribution measured by Hofstadter.8) This calculation has been done for K^- captures such that the B^{11} has been left in its ground state, and the data can be compared with the impulse model only for a restricted sample of events. In fig. 1a the B_1^{11} line (B^{11} in its first excited state) lies apart from the C^{12} line (the ground state for the B^{11} nucleus) by only a distance corresponding to 1.5 standard deviations, where we assume for σ the average error on the events. For this reason it is hard to select a sample of events to compare with the impulse model. We assumed that the events within $1.5\,\sigma$ from the C^{12} line are of type (1). In fig. 4 the M^2 and p^2 distributions of these 39 events are compared with the calculated distributions. An s-state capture seems to give a better fit than the others, but the statistics are too poor to allow any conclusion in this matter. In any case it is evident that we can explain the data without an appeal to Y_0^* (1405) production. The distributions of all the events on C^{12} (figs. 2b and 3b) could be easily obtained by a superposition of curves calculated for different excited states of B^{11}, thus shifting the M^2 peak to lower values.

In conclusion, our data do not show any evidence for Y_0^* production in C^{12} with a width of 1 MeV. If the Y_0^* (1405) had a width of $\Gamma = 1$ MeV it would travel a distance $d \approx 23$ fm before decaying. Since the B^{11} radius is ≈ 2.5 fm, the Σ and π should not have interactions inside the nucleus. Therefore with our energy resolution we should detect its production. If the Y_0^* (1405) has a 40 MeV width we should be able to see such a width in the distribution in fig. 3b. Moreover, it would go only about 1 fm before decaying. The width then would be further increased by Coulomb scattering and secondary interactions within the nucleus.

Because both excited and ground states are involved, the reaction is not well defined. Consequently, in this experiment we cannot distinguish production of Y_0^* with a width of about 20 MeV from nonresonant direct production. If the width is of this order of magnitude, we cannot measure it in any case because the mass distribution will be broadened for the above reasons.

We are deeply grateful to Dr. W. H. Barkas for his guidance and continued interest. We wish to thank Dr. M. Ferro-Luzzi and Dr. G. Alexander for many helpful discussions. We are indebted to our scanners for their painstaking measurements.

REFERENCES

1) M. Alston, L. W. Alvarez, P. Eberhard, M. Good, W. Graziano, H. Ticho, and S. Wojcicki, Phys. Rev. Letters 6 (1961) 698.

2) G. Alexander, G. R. Kalbfleisch, D. H. Miller, and G. A. Smith, Phys. Rev. Letters 8 (1962) 447.

3) M. Alston, L. W. Alvarez, M. Ferro-Luzzi, A. H. Rosenfeld, H. K. Ticho, S. G. Wojcicki, Proc. Intern. Conf. High Energy Physics, CERN, 1962, p. 311.

4) Y. Eisenberg, G. Yekutieli, P. Abrahamsson, D. Kessler, Nuovo Cimento 21 (1961) 563; Aix-en-Provence Conference Proceedings I (1961) 383.

5) Å. Frisk and A. G. Ekspong, Physics Letters 3 (1962) 27.

6) H. H. Heckman, B. L. Perkins, W. G. Simon, F. M. Smith, W. H. Barkas, Phys. Rev. 117 (1960) 544.

7) M. M. Block, Nuovo Cimento 20 (1961) 715.

8) R. Hofstadter, Rev. Mod. Phys. 28 (1956) 214.

FIGURE CAPTIONS

Fig. 1. Scatter diagram of M^2 versus p^2; (a) recoil events, (b) blob, electron, or clean events and events with more than 2 prongs. The solid lines represent kinematical relations for several kinds of nuclei (see footnote on page 3). The symbol |—⊕—| indicate the M^2 and p^2 values for Y_o^* of $M = 1405 \pm 1$ MeV produced in C^{12} and with B^{11} in its ground state. The number of events is given in parenthesis.

Fig. 2. $|\underset{\sim}{p}| = \underset{\sim}{p}_\Sigma + \underset{\sim}{p}_\pi$ distribution; (a) all 2-prong events, and (b) recoil events — — i.e., $\Sigma\pi$ production on C^{12}.

Fig. 3. Mass of $(\Sigma\pi)$ system distribution, (a) all 2-prong events and (b) $\Sigma\pi$ production on C^{12}. In (b) the dotted distribution is obtained using only events with $p > 100$ MeV/c.

Fig. 4. (a) p^2 distribution of the events within 1.5 standard deviations from the C^{12} line in fig. 1a. These are assumed to be events for which the B^{11} has been left in its ground state. (b) M^2 distribution of the same sample. The curves are calculated by an impulse model: ———— s-state capture, – – – – p-state capture (using ψ_{21}), —•—•—•— d-state capture (using ψ_{32}).

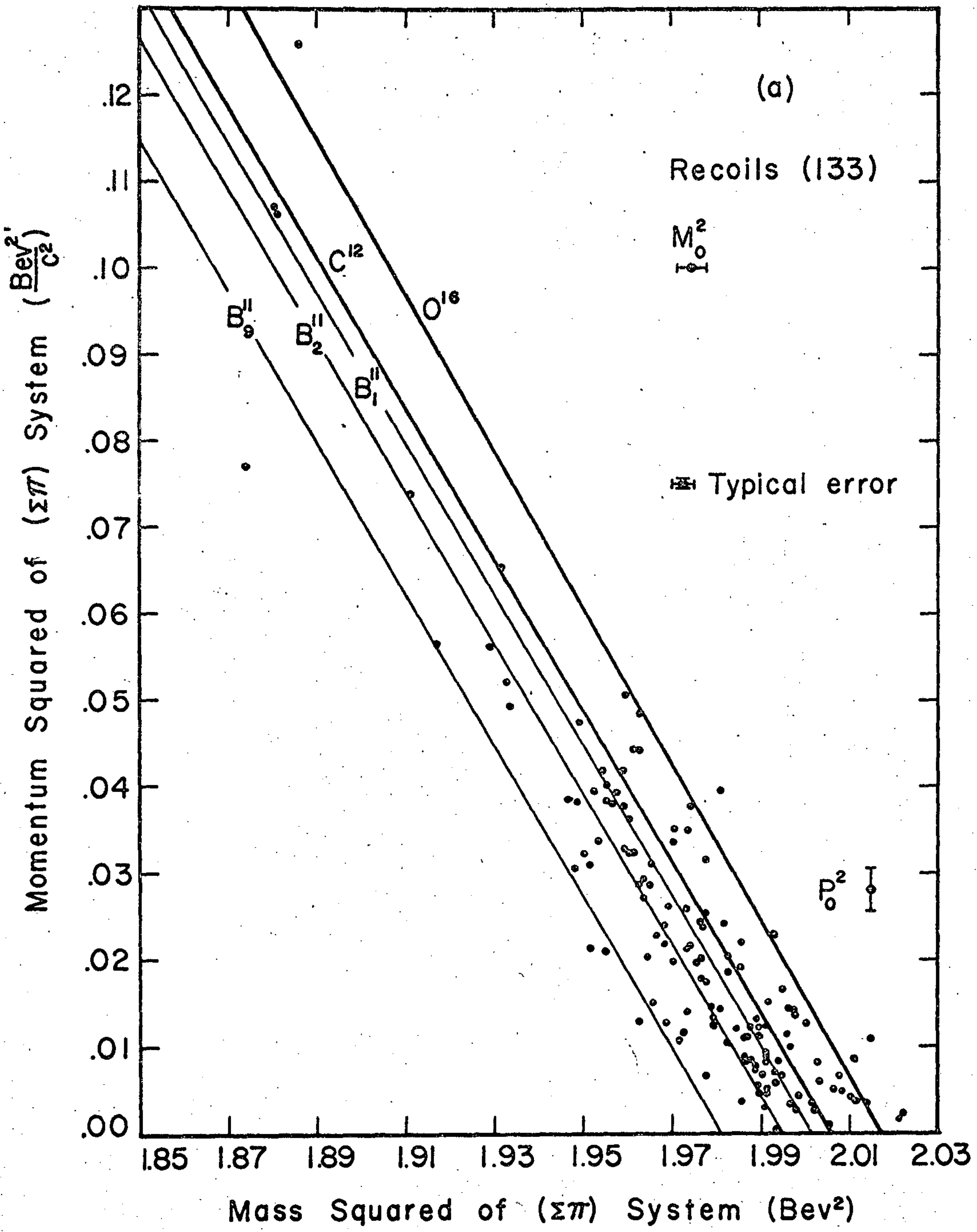

MU-30009

Fig. 1a.

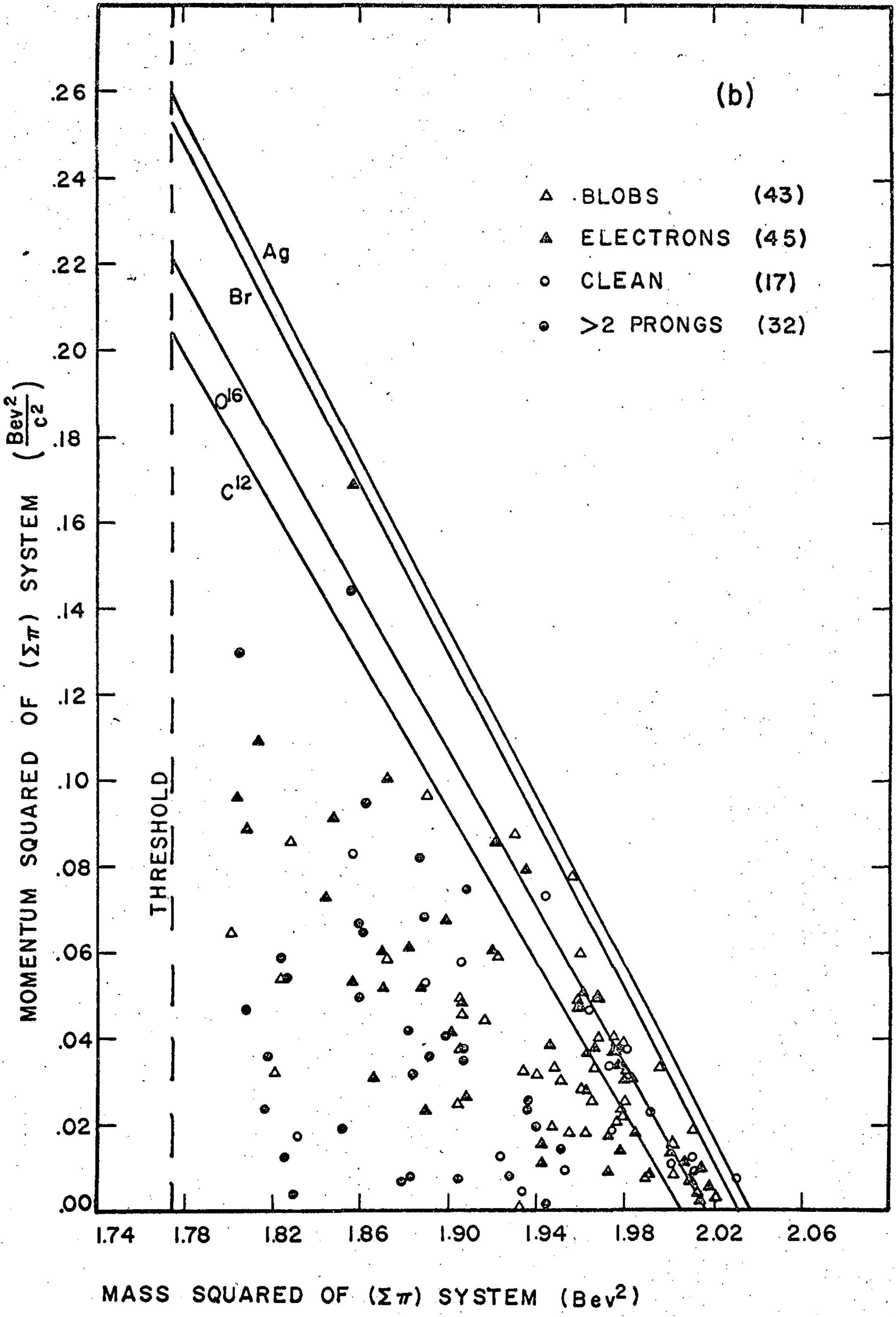

Fig. 1b.

MU-29208

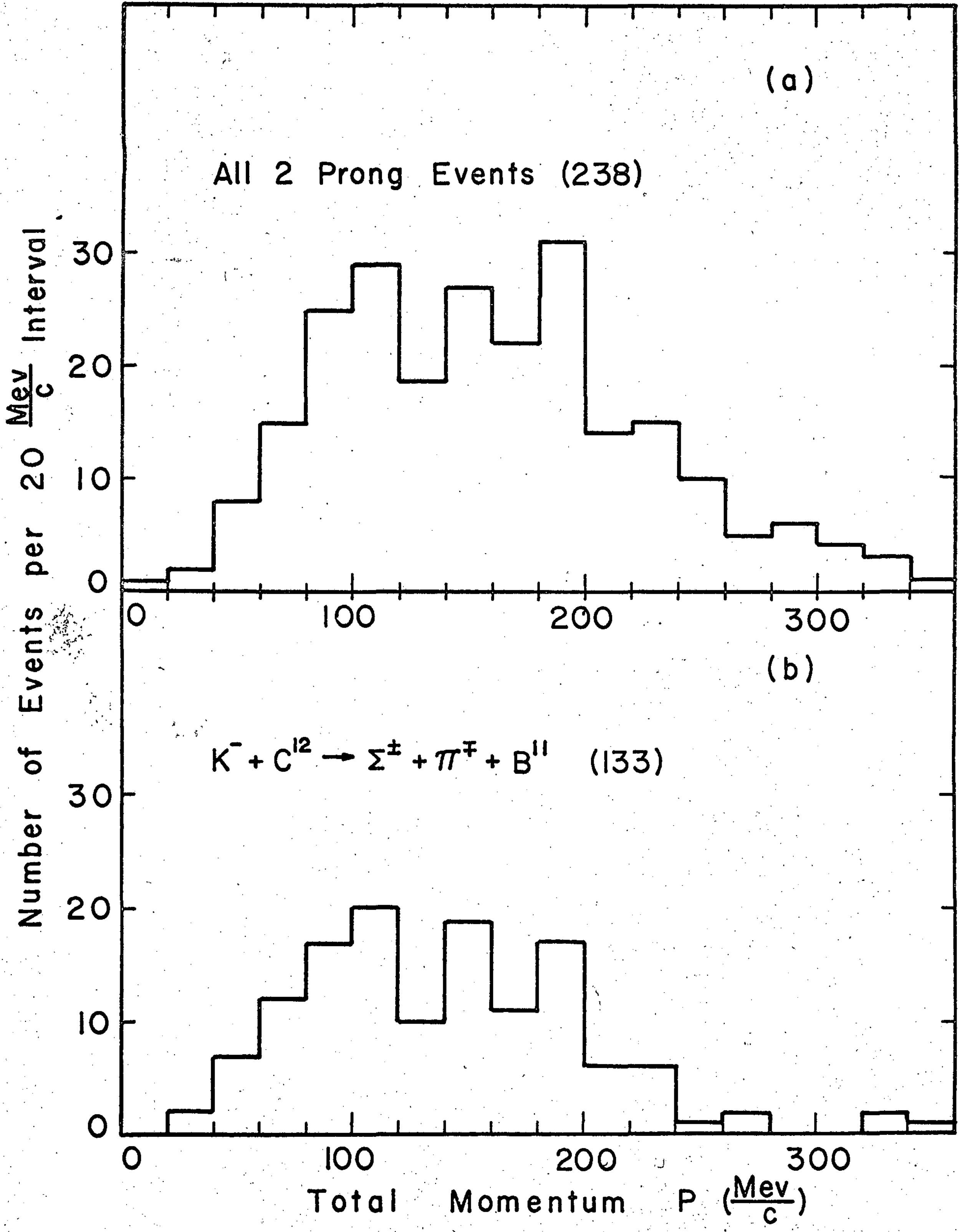

Fig. 2.

MU-30006

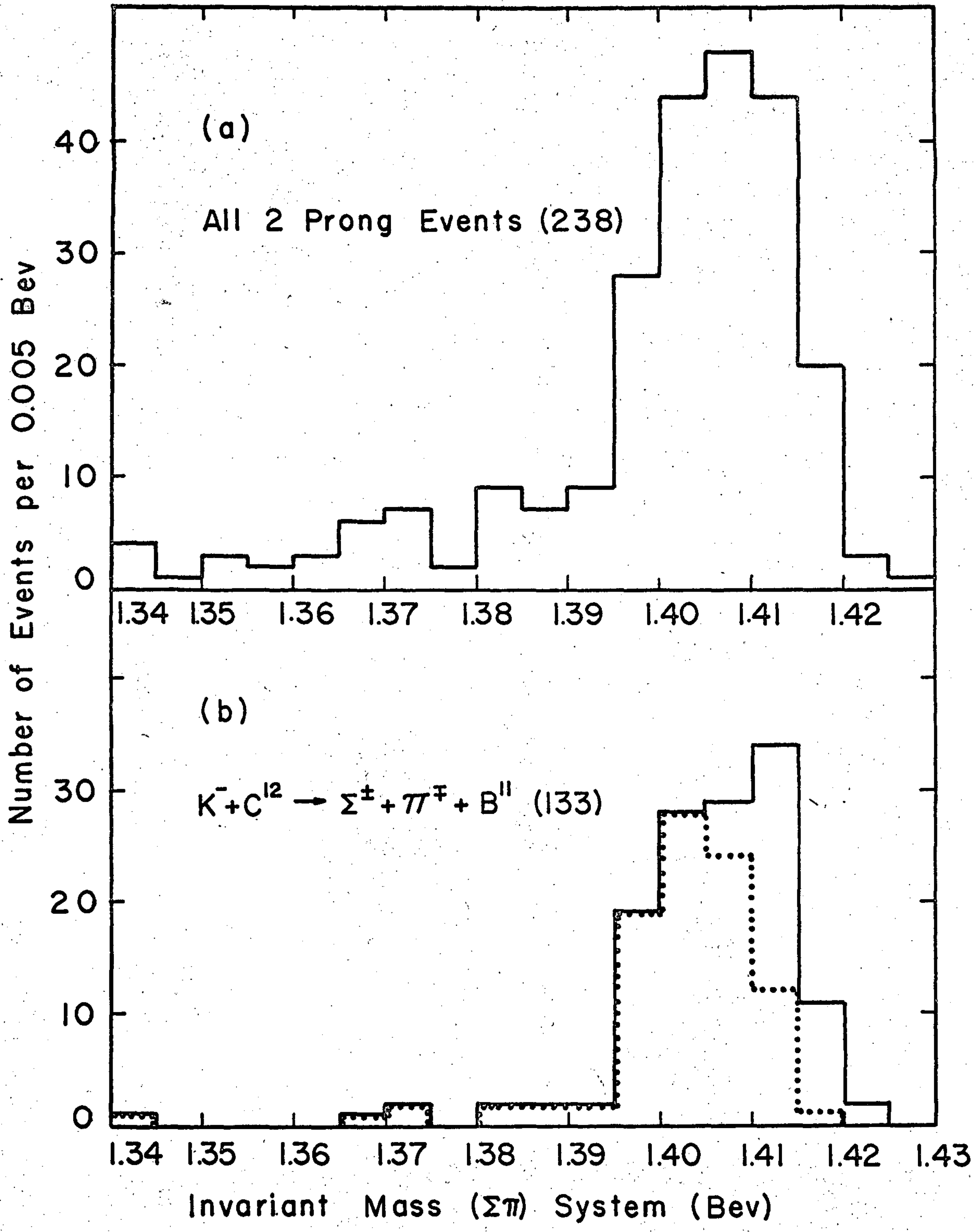

MU-30008

Fig. 3.

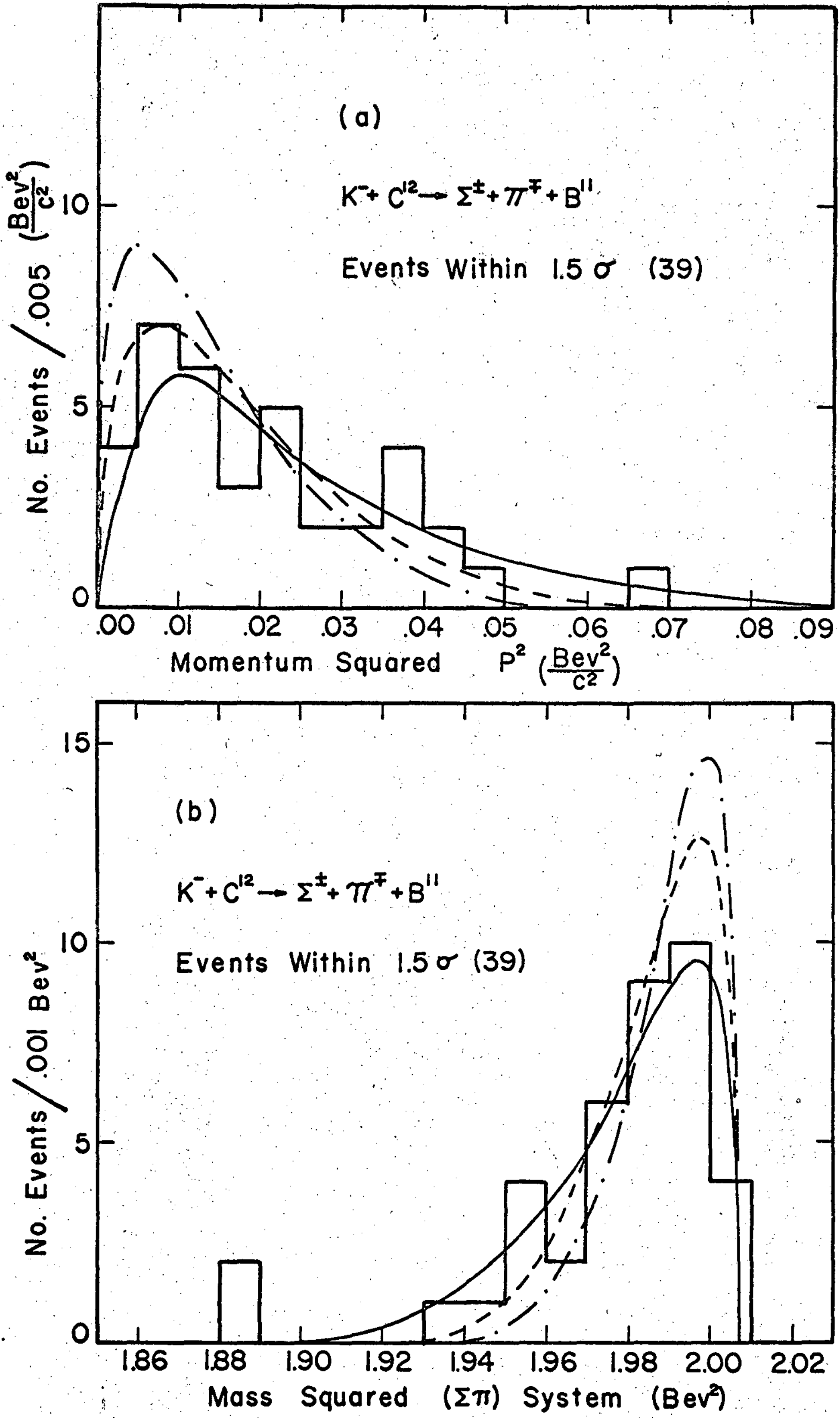

Figs. 4a and 4b.

MU-30007